Microplastic fibres from synthetic textiles: Environmental degradation and additive chemical content[☆]

Shannen T.L. Sait [a], Lisbet Sørensen [b], Stephan Kubowicz [c], Kristine Vike-Jonas [a], Susana V. Gonzalez [a], Alexandros G. Asimakopoulos [a], Andy M. Booth [b, *]

[a] Department of Chemistry, Norwegian University of Science and Technology (NTNU), NO-7491, Trondheim, Norway
[b] SINTEF Ocean, NO-7465, Trondheim, Norway
[c] SINTEF Industry, NO-0314, Oslo, Norway

ABSTRACT

Microplastic fibres (MPFs) often make up the largest fraction of microplastic pollution in aquatic environments, yet little is known about their degradative fate and persistence. This study investigates the environmentally relevant photodegradation of common MPFs: polyester (PET), polyamide (PA) and polyacrylonitrile (PAN), their respective additive chemical profile, together with their potential for additive leaching. MPFs were subject to ultraviolet (UV) exposure in seawater and freshwater media over 10 months. PET and PA MPFs showed significant fragmentation and surface changes following UV exposure, additionally PA showed evidence of chemical changes. PAN did not undergo significant photodegradation in the same exposure period. Chemicals tentatively identified in MPFs and aqueous leachates via non-target gas chromatography-mass spectrometry include monomers, UV stabilisers and degradation products. Characterisation of several bisphenols (BPs) and benzophenones (BzPs) was performed via ultraperformance liquid chromatography tandem mass spectrometry. Bisphenol A, bisphenol S and benzophenone-3 were quantified in all MPFs and wool at concentrations between 4.3 and 501 ng/g, with wool displaying the highest sum concentration of BPs and BzPs at 863 and 27 ng/g, respectively.
© 2020 The Author(s). Published by Elsevier Ltd. This is an open access article under the CC BY license (http://creativecommons.org/licenses/by/4.0/).

1. Introduction

Microplastics (MPs; 1 μm to 5 mm) are found ubiquitously across the globe in freshwater, marine and terrestrial ecosystems (Andrady, 2011). In the marine environment, microplastic fibres (MPFs) account for ~91% of MP pollution and originate from a variety of sources, including carpeting, textiles, upholstery, synthetic fishing nets and ropes (Koelmans et al., 2019; Murphy et al., 2016). Up to 60% of textiles produced globally are synthetic, with the main polymers used being polyester (PET), acrylic (polyacrylonitrile; PAN) and nylon (polyamide; PA) (Barrows et al., 2018; Lenzing, 2017). Although PET, PA and PAN garments release fibres during domestic washing, direct comparison between studies is challenging due to a lack of standardised reporting (Carney Almroth et al., 2018; Cesa et al., 2020; De Falco et al., 2018; Napper and Thompson, 2016). Many studies on fibre release documented that

PET sheds the most fibres when tested alongside other common synthetic textiles (Carney Almroth et al., 2018), with estimates that 6 million MPFs can be released from a 5 kg load of PET textiles (De Falco et al., 2018; Napper and Thompson, 2016). Although wastewater treatment plants (WWTPs) have been shown to effectively remove MPs (including MPFs) from influents (up to 99%) and retain them in activated sludge, an estimated $1 \times 10^5 - 1 \times 10^7$ MP particles are discharged in final effluent to the aquatic environment daily in some regions (Freeman et al., 2020; Koelmans et al., 2019; Mason et al., 2016; Mintenig et al., 2017; Murphy et al., 2016). Furthermore, MPs retained in sludge can also enter the aquatic environment via run-off (Corradini et al., 2019; Nizzetto et al., 2016; Zhang et al., 2020).

Owing to their durability, MPFs (and other MPs) may be considered as persistent pollutants in the environment. MPFs can be subject to several degradative processes in marine and freshwater environments, including photodegradation (UV catalysed oxidation), hydrolysis, biodegradation and mechanical degradation (Gewert et al., 2015; Zambrano et al., 2020, 2019). Photodegradation is a vital process for the environmental weathering of

polymers in aquatic environments (Andrady, 2011; Gewert et al., 2015). Although available data concerning the environmental degradation of MPFs is scarce, they are expected to degrade similarly to other MPs. Qualitative signs of photodegradation include polymer discoloration and surface cracking (Da Costa et al., 2018; Gewert et al., 2015). These degradation processes increase the polymer surface area and cause embrittlement, which in combination with mechanical forces (e.g. wind, waves, etc), result in increasing fragmentation, and ultimately, mineralisation by microbes to CO_2 (Da Costa et al., 2018; Gewert et al., 2015).

Chemical additives are added to polymers to impart desirable physical, chemical and even biological (e.g. antimicrobial) properties, improve performance and increase functionality (Chequer et al., 2013; Cole, 2016; Darbra et al., 2012). These chemicals are typically not covalently bonded to the polymer matrix and are therefore expected to leach more readily into the aquatic environment (Hermabessiere et al., 2017). Degradation is expected to further increase the potential for additive chemical leaching (Wang et al., 2018). Studies indicate chemical leachates from pristine and UV-weathered plastics can lead to a range of toxicological responses, including oxidative stress activation and increased induction in algae and cells (Capolupo et al., 2020; Rummel et al., 2019). As little is known about the occurrence of potentially toxic chemicals in textiles, it is therefore necessary to characterise which additives are present in MPFs and how they leach into aqueous media under conditions that simulate environmental degradation processes.

Bisphenols (BPs) and benzophenone UV-filters (BP-UV filters; BzPs) are two high production volume additive chemicals (Asimakopoulos et al., 2014b, 2014a). BPs are widely used in the manufacture of various plastics and include several analogues; the most prominent being bisphenol A (BPA) (Asimakopoulos et al., 2014a). In textile manufacturing, BPA is used as a coating and intermediate chemical in the manufacture of dyes and antioxidants and was recently detected in a range of garments (Wang et al., 2019; Xue et al., 2017). While BPA is extensively researched, concentrations of other BPs and possible exposure pathways remain largely understudied. BzPs are frequently applied as UV filters in plastic products to prevent or reduce UV-induced degradation (Asimakopoulos et al., 2014a) and are used for this reason in the textile industry to increase product lifetime (Xue et al., 2017).

The current study investigates the long-term environmental degradation of the commercially important MPFs, including PET, PA and PAN. The objectives of the study were to: i) investigate UV degradation of MPFs in marine and freshwater environments using optimised UV exposure conditions that represent environmental conditions; ii) assess additive leaching under different environmental conditions; and iii) investigate the occurrence of selected multiresidue plasticizers, BPs and BzPs in MPFs and their aqueous leachates.

2. Materials and methods

2.1. Chemicals and materials

Methanol (MeOH) was purchased from Merk (Darmstadt, Germany), dichloromethane (DCM) from Rathburn (UK), n-hexane and isopropanol (IPA) from Fluka Analytical (Steinheim, Germany) and ethyl acetate (EtOAc) and ammonium acetate from Sigma-Aldrich (Steinheim, Germany). A 37% (v/v) solution of hydrochloric acid (HCl) and sodium sulphate (Na_2SO_4) were purchased from Merck (Darmstadt, Germany). BP and BzP analytical standards were purchased from Sigma-Aldrich (Steinheim, Germany) (Supplementary Information, SI). Isotopically labelled internal standards were purchased from Cambridge Isotope Laboratories, Inc. (Massachusetts,

United States) (SI). Deuterated polycyclic aromatic hydrocarbon (PAH) standards were purchased from Chiron AS (Trondheim, Norway). Colourless Richard-Allan Scientific™ Neg-50™ frozen section medium (glycol solution) was purchased from Thermo Fischer Scientific (Massachusetts, United States). Natural seawater was collected from a depth of 90 m in the Trondheim fjord and sterile filtered (0.22 μm, Sterivex®) prior to use. Freshwater media (TG 201) was prepared according to OECD Guideline 2011 (OECD, 2011) as detailed in the SI.

Polyester (PET), polyamide (PA), polyacrylonitrile (PAN) and treated wool were supplied by commercial textile producers (Table S1). Wool is a popular fibre for use in textiles, especially in colder climates and was selected as a natural fibre reference in the additive chemical profiling studies. MPFs from the synthetic yarns were prepared with minor modifications according to Cole (2016). Briefly, yarns were wrapped around a custom-made spool (Fig. S1), covered in glycol medium and kept frozen at −80 °C before being sectioned to 1−2.5 mm using a scalpel. Sectioned MPFs were collected, rinsed with Milli-Q water, filtered (0.45 μm cellulose filters, MF-Millipore) and dried at 40 °C for 75 h in covered Petri glass dishes.

2.2. Exposing MPFs to UV light

MPF UV exposure experiments were performed in artificial freshwater media or natural seawater using an Atlas Suntest CPS + instrument fitted with a Xenon lamp (1500 W) and daylight filter, with intensity regulated at 300−400 nm. Irradiation was conducted at 65 W/m^2 and the temperature in the exposure chamber was maintained at 24 ± 3 °C. Control samples were kept in the dark at room temperature (20 ± 1 °C). Sampling was conducted after 153 (~5 months) and 291 days (~10 months), which corresponded to ~1452 days (4 years) and ~2761 days (7.5 years) of mean European solar irradiance exposure, respectively (details in SI) (Gewert et al., 2018). MPFs were isolated by filtration (40 μm, Corning® sterile nylon cell strainer), rinsed thoroughly with Milli-Q water and dried at 40 °C for 76 h. A detailed description of the methodological approach is provided in the SI. The extent of UV-induced MPF degradation was assessed using a combination of light microscopy, scanning electron microscopy (SEM) and attenuated total reflectance-Fourier transform infrared spectroscopy (ATR-FTIR) to investigate changes in fibre length (fragmentation), surface morphology and polymer chemistry.

2.3. Physical characterisation of MPFs

All light microscopy was performed using a Nikon Eclipse E200 microscope and post-processed in ImageJ® (Schneider et al., 2012). The scale was set according to the objective lens used and calibrated using a stage micrometre slide. The length distribution of the sectioned pristine MPFs was determined, as shown in the supplementary information (SI, Fig. S4). The length distributions of UV-exposed and control MPFs were likewise determined using the same approach, where MPF lengths were measured manually using the measure function in ImageJ®. At least 30 MPFs were measured in each sample, with up to 250 individual fibres measured where images contained numerous MPFs (e.g. after UV exposure). Prior to statistical analysis, 30 measurements from each data set were randomly selected using a random number generator to avoid sampling bias ("Random Integer Generator," 1998).

Differences in the surface structure of the pristine, degraded and control MPF samples were qualitatively studied using scanning electron microscopy (SEM). All SEM was performed using a Zeiss Ultra 55LE field emission SEM (FEG-SEM, Carl Zeiss AG), with samples thinly coated in a layer of gold (Au) via low vacuum

sputtering (Edwards S150b Gold sputter coater, Edwards, UK) to minimise charge build-up. SEM images were captured at 10 mm working distance and a 2−10 kV accelerating voltage. Images were captured at 3 different magnifications (x100, x500 and x2000) to allow for both an overview of the sample and a detailed examination of the surface morphology. Scale bars were added in ImageJ®.

2.4. Polymer composition of MPFs

To investigate changes in polymer composition following UV-light exposure, ATR-FTIR was performed using a Bruker ALPHA ATR-FTIR spectrometer equipped with a diamond crystal. For each sample, three spectra were recorded at 4 cm^{-1} resolution with 47 scans (700−4000 cm^{-1}). Background subtraction, baseline correction and normalisation were performed in OPUS. The spectra were investigated with respect to changes in peak and relative intensities. Carbonyl index is a measure of photodegradation and has been employed in degradative studies on polyethylene and polypropylene, as well as characterisation of weathering in environmental samples (Allen and Edge, 1992; Rouillon et al., 2016; Sathish et al., 2019). The carbonyl index in the current study was calculated as the peak intensity ratio between a carbonyl peak at ~1700 cm^{-1} and a specific reference peak unique to each textile type (Karlsson et al., 2018). For PET this was 1407 cm^{-1} (νC=C), for PA this was 932 cm^{-1} (νC-CO) and for PAN this was 1360 cm^{-1} (CH bend) (Porubská et al., 2012).

2.5. Aqueous leachate studies

Short-term aqueous leachates of PET, PA and PAN MPFs and wool were obtained by shaking 350 mg of 5 mm fibres in 35 mL (10 mg MPF mL^{-1}) of filtered seawater (5 and 20 °C) and freshwater media (20 °C). Blank control samples without MPFs were included. The two different seawater temperatures chosen to reflect sea temperatures found in both temperate regions (20 °C) and more polar regions (5 °C). Samples were shaken on a Gerhardt shaking table (horizontal motion) at ~2−3 Hz. After 14 days, leachate samples (2 mL) were isolated from MPFs (40 μm, Corning® sterile nylon cell strainer) for non-target chemical profiling and target analysis of BPs and BzPs. Long-term aqueous leachates of each MPF were produced and sampled as part of the UV exposure study described above (section 2.2) but generated using lower MPF concentrations (1 mg mL^{-1}) and sample volumes (10 mL) than the short-term study.

2.6. Non-target chemical profiling

Non-target chemical profiling was conducted both on the pristine MPFs and on the freshwater and seawater leachate solutions (from both long-term and short-term studies). To determine the chemicals present in the pristine PET, PA, PAN and wool yarns, samples were prepared and analysed according to Cole et al. (2019). Details of the MPF and leachate extraction and sample preparation approach are presented in the SI. All non-target samples were analysed using an Agilent 7890A gas chromatograph (GC) equipped with an Agilent 5975C mass spectrometer (MS). The inlet was set at 250 °C, the transfer line at 300 °C, the ion source at 230 °C and the quadrupole at 150 °C. The carrier gas was helium with a constant flow rate of 1.1 mL/min. The sample (1 μL) was introduced via pulsed splitless injection. An Agilent DB5MS ultra-inert column (30 m, 0.25 μm film thickness, 0.25 mm i.d.) was used and the GC oven was held at 40 °C (2 min), ramped by 6 °C/min to 320 °C for a 20 min hold. After a 12 min hold time, mass spectra were recorded

in full scan mode (50−500 m/z).

2.7. Analysis of bisphenols and benzophenone UV filters

Preparation of pristine MPFs and aqueous leachates (UV and short-term 14-day leachates) for the analysis of BPs and BzPs was performed using solid-liquid extraction (SLE) and liquid-liquid extraction (LLE). Details of the MPF and leachate extraction and sample preparation approach are presented in the SI. Ultra-performance liquid chromatography tandem mass spectrometry (UPLC-MS/MS) analysis was conducted according to a modified approach previously reported by Asimakopoulos et al. (2014a, 2014b). Specific details concerning the UPLC-MS/MS analysis method, including quality assurance and quality control measures are available in the SI (Methods, Tables S2−S6 and Figs. S2−S3).

2.8. Data analysis and statistical treatment

For non-target analysis, GC chromatograms and mass spectra were recorded in ChemStation software and MassHunter Unknowns Analysis software was applied to the raw data files for deconvolution and tentative identification of analytes. Output files were exported to. csv format for further processing using R (R Core Team, 2017). In R, chemicals were filtered based on their presence in at least 2 of 3 replicates and when >90% match to NIST 2017 library mass spectra was established. For the target analysis of BPs and BzPs, UPLC-MS/MS data were acquired and processed using Intellistart, MassLynx and TargetLynx software packages (Waters, Milford, U.S.), with further processing in Excel (Microsoft, 2018). All statistical analysis was conducted in GraphPad Prism (v. 8.02). For UV-induced fragmentation data, a Kruskal-Wallis test was performed within MPF groups (PET, PA, PAN) due to non-normal data. For pairwise comparisons, Dunn's multiple comparison tests were employed. The statistical significance was set at $P < 0.05$.

2.9. Quality assurance and quality control (QA/QC)

Several QA/QC measures were implemented in the experimental approach. First, all solvents used were analytical grade. All glassware was pre-cleaned using detergent, rinsed thoroughly with MilliQ water and then heat treated (>400 °C) to remove organic impurities. Potential sources of additive contamination were minimised by avoiding the use of any plastic equipment and using only pre-washed glass and metal items. All filters were solvent rinsed prior to use. To reduce potential issues with contamination by plastic additives from sources other than the MPFs, the additive chemical profile was first determined in the pristine MPF materials and only those chemicals identified by strong mass spectral matches or suspected degradation products were targeted for analysis in the leachate studies. For BzP and BP analysis, samples were prepared in pre-cleaned polypropylene tubes and any contamination arising from laboratory materials and solvents was evaluated by the analysis of procedural blanks. For each batch of 10 samples analysed, one procedural blank was analysed simultaneously, and a calibration check standard was injected after every 25 samples as a check for drift in instrumental sensitivity. In addition, a methanol blank (LC-MS analysis) was injected after every two samples and a DCM blank (GC-MS analysis) was injected after every five samples as checks for carry-over between samples.

3. Results and discussion

3.1. Fragmentation of fibres following UV-light exposure

After both 5 and 10 months of exposure, fragmentation was

observed for the PET and PA fibres, but not for PAN. Changes in the mean MPF length of UV exposed samples in seawater are discussed below, while median changes in MPF length are presented in the SI (Table S7). Black PET MPFs significantly decreased in length (Kruskal-Wallis; $P < 0.0001$; Fig. 1A) from a mean value of 1303 μm−217 μm (83.4% decrease) and 140 μm (89.3% decrease) after 5 and 10 months UV exposure, respectively. Although there was a slight decrease in mean MPF length from 5 to 10 months, this was not significant (Kruskal-Wallis; $P > 0.99$). White PET also displayed a significant decrease in MPF length (Kruskal-Wallis; $P < 0.0001$; Fig. 1B) from a mean value of 1388 μm−80.2 μm (94.2% decrease) and 63.0 μm (95.5% decrease) after 5 and 10 months UV exposure. Similarly, PA exhibited a significant decrease in MPF length (Kruskal-Wallis; $P < 0.0001$; Fig. 1E) from a mean value of 1453 μm−550 μm (62.2% decrease) and 373 μm (74.3% decrease) after 5 and 10 months UV exposure, respectively. The change in length from 5 to 10 months was insignificant (Kruskal-Wallis;

$P > 0.99$). In contrast to PET and PA, PAN MPFs (Fig. 1C and D) showed no significant change in mean MPF length after 10 months UV exposure. No significant fragmentation or change in mean fibre length was observed in any dark control sample over the duration of the study. Furthermore, no significant differences were observed between seawater and freshwater exposure media for any MPF materials.

UV-light induced fragmentation suggests that PET and PA can degrade more readily in surface or shallow waters in aquatic environments that receive sunlight. In contrast, PAN is likely to be more persistent under the same conditions. It should be noted that all MPFs investigated in the current study are denser than seawater and freshwater and that UV exposure will not be a viable degradation mechanism once they have settled below the photic zone. The photodegradation of white PET resulted in increased brittleness and yellowing (Fig. S5), which is in line with previous observations (Andrady, 2003). While an increase in PA brittleness was
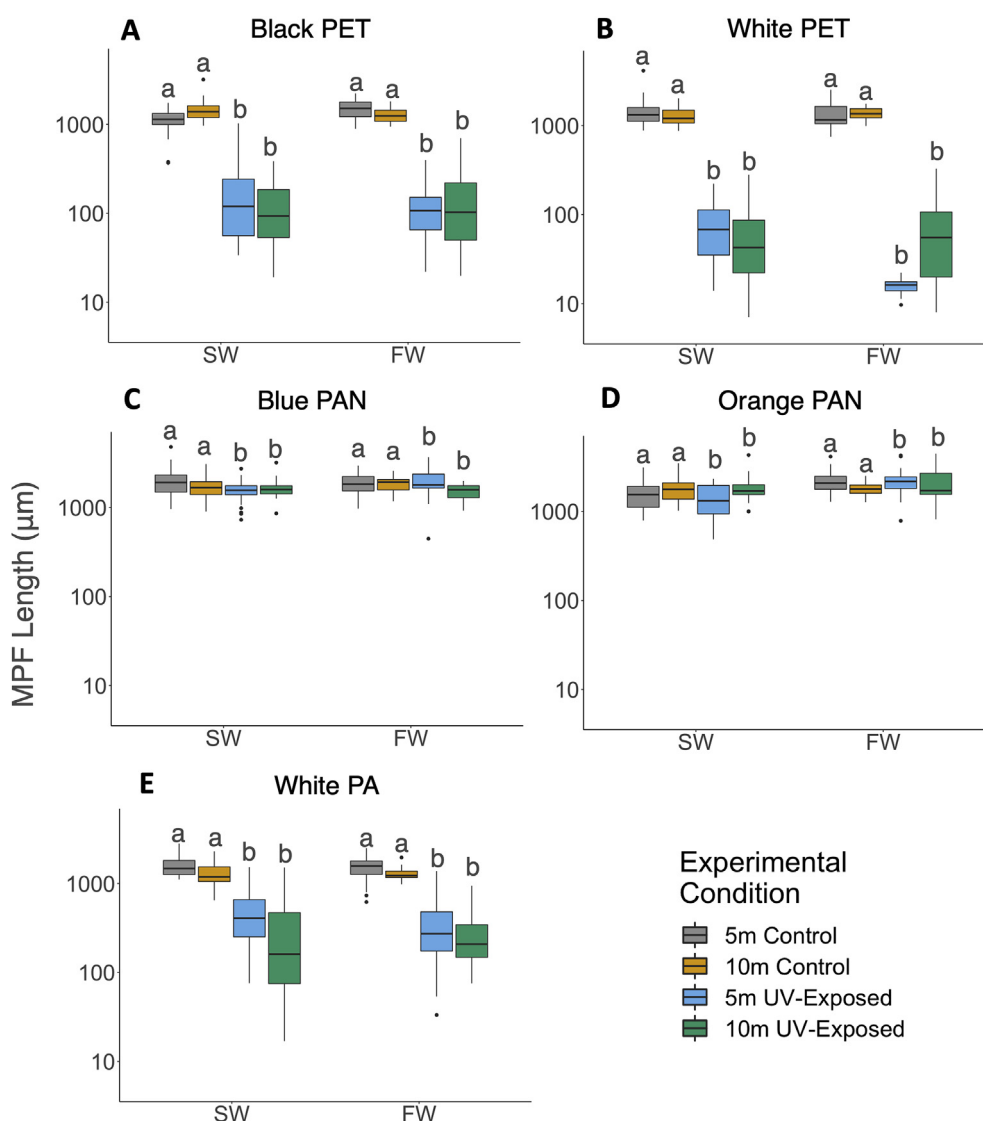

Fig. 1. Change in length (μm) of black PET (A), white PET (B), blue PAN (C), orange PAN (D) and white PA (E) MPFs after 5- and 10-months simulated UV exposure and in dark controls (no UV) in seawater (SW) and freshwater (FW). Statistical analysis was performed within groups: PET, PAN and PA, respectively. Boxplots: median and 25:75 percentiles; bars: minima and maxima; black dots represent outliers. Lowercase letters (a, b) denote significant difference in MPF length for each material. n = 30 for all samples. (For interpretation of the references to color in this figure legend, the reader is referred to the Web version of this article.)

evidenced by the reduction in mean MPF length; no yellowing was observed following UV irradiation. This may be attributed to the use of anti-yellowing additive chemicals in the manufacture of polyamides (Andrady, 2003; Weedon and Decaprio, 1971). PAN can undergo photodegradation as demonstrated in laboratory-based studies, however environmental photodegradation has not been previously assessed (Aggour and Aziz, 2000; Jellinek and Bastien, n.d.; Jellinek and Schlueter, 1960). The analogous changes in MPF length between exposure media in the current study indicated that salinity does not appear to significantly influence UV induced fragmentation.

3.2. Changes in MPF surface morphology

Black PET MPFs displayed orthogonal surface microcracking after 5 months of UV irradiation, with an apparent increase in abundance after 10 months (Fig. 2A). Interestingly, SEM images of white PET presented the formation of small holes or dimples along the surface after 5 months of UV exposure (Fig. 2B) rather than the microcracks observed for black PET. After 10 months of UV irradiation, the surface morphology of white PET appeared to be similar to that after 5 months of exposure, but with the presence of visible orthogonal microcracking. The appearance of surface microcracks infers an increase in sample brittleness, which may indicate further photodegradation. Deep holes and crevices were evident in the surface of PA after 5 months of UV exposure (Fig. 2C), which became deeper and more distinct after 10 months. SEM images of blue and orange PAN showed little evidence of surface degradation. Minute holes were visible on the surface of blue PAN after 5 months of UV irradiation (Fig. 2D), increasing in both frequency and size after 10 months, implying the initial stages of degradation may be proceeding. SEM images of orange PAN MPFs showed little change in surface morphology after 5 and 10 months of UV exposure (Fig. 2E). It is evident from SEM micrographs that the MPF surface did not photodegrade homogenously. It was uncertain why this occurred but may be associated with nanoscale defects and uneven distribution of additive chemicals (e.g. UV stabilisers). Comparable observations were seen in MPFs exposed in freshwater media (Figs. S6–S10), apart from PA which appeared to show a lower degree of change in surface morphology in freshwater media relative to seawater (Fig. S8).

Cracking or microcracking is often described in the UV degradation of PET, however the formation of small holes observed on the surface of white PET MPFs was not previously reported in laboratory photodegradation studies (Armstrong et al., 1995). Small holes have been observed on the surface of polycarbonate films after hydrolytic degradation studies (Chandure et al., 2014). This can indicate that hydrolysis is occurring concurrently with UV photodegradation in the current study. Despite a thorough literature search, the extent of the UV-initiated surface morphology changes observed in PA in this study are not reported previously. Surface microcracking was previously observed in photodegraded PA films, but the formation of deep fissures was not described (Ksouri and Haddar, 2018). In a study of field samples, formation of irregular pores, pits and cracks on the surface of PA and PET fibres similar to the ones observed in the current study was identified and related to environmental degradation (Sathish et al., 2019). This drastic UV-induced transformation in the surface morphology of PA suggests that nano-sized particles can be a product of the environmental weathering of MPFs, especially when combined with mechanical forces. This is a potentially significant finding, as nano-sized fragments are considered more bioavailable and can translocate into biological tissues (Dawson et al., 2018; Revel et al., 2018). Future studies on the potential for MPF nano-fragmentation under environmentally relevant exposure conditions are therefore recommended. While PAN MPFs did not undergo notable changes of their surface morphology, the blue PAN MPFs did present greater variations than the orange PAN MPFs. It was hypothesised this may be associated with differences in the additive chemical composition of the two materials, including the colorant or dye used.

MPF photodegradation rates depend on many intrinsic physicochemical properties and extrinsic environmental factors. While PET and PA showed a greater extent of degradation in this study, these materials may not be illustrative of all types of PET, PA and PAN used in textiles or found in the environment. The physicochemical properties of the materials, e.g. the presence of UV
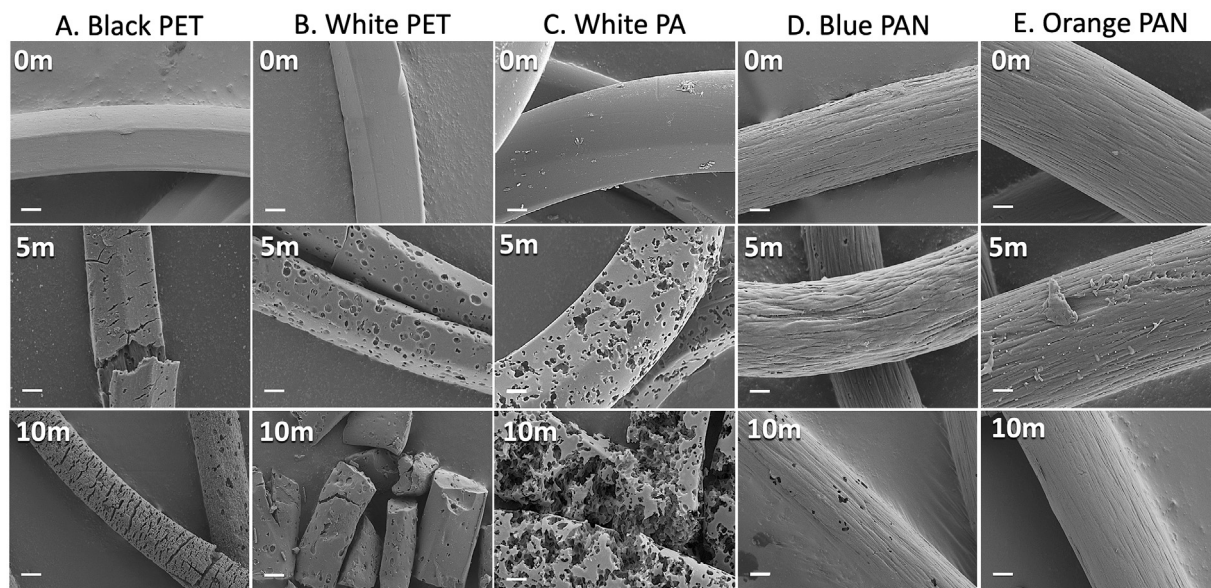

Fig. 2. SEM micrographs showing changes in surface morphology before (0m) and after 5- (5m) and 10-month (10m) UV exposure in seawater. Images are taken at 2000x magnification. Where A is black PET, B is white PET, C is white PA, D is blue PAN and E is orange PAN. Scale bars represents 5 μm.

stabilisers and antioxidants, would hinder the rate of environmental degradation, prolonging environmental lifetimes. In contrast, the presence of other additive chemicals could increase the susceptibility of a particular material to degradation processes (Deterre et al., 2014).

3.3. Changes in polymer chemistry

The pristine FTIR spectrum of PET was previously characterised (Ioakeimidis et al., 2016; Parvinzadeh and Ebrahimi, 2011; Vahur et al., 2016). A decrease in absorbance was observed at peaks 1711 (vC=O), 1238 (vC-O) and 1090 cm^{-1} (vC-O) in UV exposed black PET fibres (Fig. S11) relative to controls. Similar to black PET, a decrease in absorbance in white PET was observed at peaks 1711 (vC=O), 1238 (vC-O) and 1090 cm^{-1} (vC-O) in UV-irradiated samples (Fig. S13) relative to pristine and control samples. Observed decreases in absorbance can indicate UV-induced oxidation. The appearance of a band at 3315 cm^{-1} for white PET in seawater after 5 months of UV exposure was likely associated with insufficient rinsing of this material prior to analysis, as residual salts could result in moderate to strong peaks in the 3000-3500 cm^{-1} range, potentially corresponding to −NH (Patty et al., 2017). The absence of this peak in freshwater samples (Fig. S14) further supports this hypothesis.

The FTIR spectrum of pristine PA was characterised previously (Porubská et al., 2012; Vahur et al., 2016). UV-exposed PA displayed increased absorption relative to the dark control at peaks 3295 cm^{-1} (vN-H), 2921 cm^{-1} (vC-H), 1631 cm^{-1} (vC=O) and 1530 cm^{-1} (δ_sN-H) (Fig. S15). The increased absorption in UV-exposed PA was consistent with a study examining the accelerated photodegradation of PA and is likely attributed to imide formation from photodegradation (Thanki and Singh, 1998).

The FTIR spectrum of pristine PAN was characterised in previous studies (Ribeiro et al., 2015; Vahur et al., 2016). Both blue and orange PAN showed no shifts in absorbance associated with UV irradiation (Figs. S17 and S19). However, the formation of peaks at ~1600 cm^{-1} and increased intensity at 2915 and 2446 cm^{-1} in dark controls were attributed to the presence of bacteria. This was further supported by the absence of these peaks in UV irradiated samples as UV-light is a known bacterial growth inhibitor.[50]

After 5 months of UV exposure, PET MPFs showed decreases in carbonyl indices from 2.95 for the pristine material (t = 0) to 1.44 and 1.00 for PET in freshwater and seawater, respectively (Fig. S21). This is consistent with the observed decreases in absorbance in the FTIR spectra (Fig. S11 and Fig. S12) and changes in the surface morphology and degree of fragmentation. Nevertheless, there was no clear temporal trend as carbonyl indices did not decrease after 10 months, suggesting that further changes in surface chemistry did not occur. PA MPFs displayed increased carbonyl indices after 5 months of UV exposure (Figs. S15 and S16), increasing from 1.17 for the pristine material (t = 0) to 2.11 and 7.69 for PA in freshwater and seawater, respectively. This is consistent with the observed increases in absorbance in the FTIR spectra (Fig. S23), the observed changes in surface morphology and the degree of fragmentation. Carbonyl indices of PA in freshwater and seawater increased after 10 months, indicating a temporal pattern of increasing degradation. In the case of the PAN MPFs, no obvious trends were identified in the FTIR spectra or the calculated carbonyl indices (Figs. S24 and S25) after 5 and 10 months of UV exposure, which is consistent with the absence of changes in surface morphology and lack of fragmentation.

3.4. Non-target chemical profiling

A combination of non-target analysis by GC-MS and targeted analysis of BPs and BzPs by UPLC-MS/MS were used as they are complementary to one another. Furthermore, GC-MS is considered more suitable for non-target analysis due to the extensive mass spectral libraries available. A range of chemicals, including monomers, degradation products and UV stabilisers were tentatively identified in the pristine MP and wool fibres, 5- and 10-month UV leachates and short term 14-day leachates (Tables S9−S12). In general, tentatively identified chemicals were unique to each MPF type. The two exceptions to this were (i) nonanal identified in both PET and wool, and (ii) ethyl 4-ethoxybenzoate present in both PAN and wool. Nonanal is used in perfumes but other uses cannot be excluded (Arctander, 2019). Ethyl 4-ethoxybenzoate is a known plastic additive and used during the manufacture of a range of plastics, which can explain its occurrence in PAN (National Center for Biotechnology Information PubChem Database, n.d.). Its presence in wool can be associated with industrial processing on the same machinery as synthetic textiles or could be an external source of contamination. A considerable number of identified chemicals could not be classified based on known uses. It is evident from this non-target approach that a considerable proportion of chemical compounds are either not available in spectral databases or very little literature exists about their use and potential environmental impact. Further investigation of leachates using high-resolution MS could help elucidate the structure and identity of chemicals present in plastic and plastic leachates, but progress on the automated data analysis front is also needed to handle the complexity of these datasets for high-throughput characterisation (Zimmermann et al., 2019).

Non-target chemical profiling of the aqueous media from 5- and 10-month UV exposure studies tentatively identified chemicals that leached out during environmental photodegradation (in addition to potential degradation products). Potential degradation products were identified in PET MPFs after UV exposure, where all presented similar structures to the starting monomer and were not present in pristine PET MPFs (Table S9). Acetophenone was identified as a chemical in both pristine PET fibres and UV leachates. As acetophenone is used as a catalyst in polymerisation this likely accounts for its presence in both PET MPFs and their UV leachates (Frick et al., 2014). Caprolactam was the only chemical identified in both pristine PA fibres and respective UV leachates, which was attributed to its use as a starting material in the polymerisation of PA (Table S10) (Zhang et al., 2019). Furthermore, a potential degradation product (2-methyl-2-butenal) was identified in leachates after 10 months UV exposure. No chemicals were identified in both pristine PAN MPFs and UV leachates, although ethyl 4-ethoxybenzoate was identified in the 10-month UV leachates (Table S11). Due to the size constraints of the UV exposure chamber, wool was not included in the UV studies and as such the potential for additive leaching from wool could not be assessed. Generally, there were few chemicals identified in both pristine MPFs and UV leachates. This can be attributed to relatively low fibre concentrations (1 mg mL^{-1}), combined with the photodegradation of any leached chemicals under the harsh and long exposure conditions.

To determine if additive chemicals present in the MPFs have the potential to leach into aquatic environments, 14-day leachate studies were conducted with high MPF concentrations (10 mg mL^{-1}). For PET, no chemicals identified in pristine materials were determined in the 14-day leachates. For PA MPFs, caprolactam and cyclopentanone, 2 of the 3 chemicals tentatively identified in

pristine PA MPFs were also present in the 14-day seawater leachates, but not the freshwater leachates. In pristine PAN MPFs, 2 out of 6 tentatively identified chemicals (ethyl 4-ethoxybenzoate and 2,2,5-trimethylhexane-3,4-dione) were also present in the 14-day freshwater leachates. For the wool fibre, 3 out of the 9 tentatively identified chemicals (cyclobutane-1,1-dicarboxamide N,N′-di-benzoyloxy-; ethyl 4-ethoxybenzoate and oxalic acid allyl nonyl ester) were also present in aqueous leachates. Based on this study, additive leaching from MPFs can be impacted by relative salinity. The non-target approach indicated that chemical residues could leach out of certain MPFs and wool in the environment.

3.5. Occurrence of bisphenols and benzophenones in MPFs and leachates

The concentration of BPs and BzPs in the pristine MPFs and wool fibres are presented in Fig. 3 and Table S8. BPA was the most abundant BP across all samples, with median concentrations ranging between 25.4 (PET white) and 501 ng/g (wool). Bisphenol S (BPS) was the second most abundant BP found in all MPFs and wool, ranging between 0.29 (PAN orange) and 1.96 ng/g (wool). Interestingly, wool showed the highest total BP content at 560 ng/g, followed by PAN blue (165 ng/g), PAN orange (105 ng/g), PA (73.6 ng/g), PET black (87.8 ng/g) and PET white (25.8 ng/g). Wool also contained the highest prevalence of BPs (4 in total: BPA, BPS, bisphenol AP (BPAP) and bisphenol F (BPF)). Of the BP-UV filters, benzophenone-3 (BzP-3) was found at the highest concentration across all fibre types. The lowest median concentrations of BzP-3 were found in blue and orange PAN at 4.33 and 7.77 ng/g, respectively. Higher, but similar median BzP-3 concentrations were found in PA, white PET, black PET and wool at 13.6, 17.0, 17.9, and 20.7 ng/g, respectively. Similar to BPs, wool showed the highest total BzP content at 26.9 ng/g, followed by PET black (18.7 ng/g), PET white (17.1 ng/g), PA (13.1 ng/g), PAN orange (8.5 ng/g) and PAN blue (4.97 ng/g). There was no noteworthy difference in the BzP chemical profiles between the 6 materials, with each containing varying levels of benzophenone-1 (BzP-1), BzP-3 and 4-hydroxybenzophenone (4-OH-BzP), except for PA which contained only BzP-3.

In general, the findings of this study agree with previous reports of BP and BzP content in textiles. In recent studies examining the occurrence of BPs and BzPs in children's textiles, BPA, BPS and BzP-3 were also the most prominent chemicals in MPFs and wool (Freire et al., 2019; Xue et al., 2017). Higher median concentrations of BPA and BPS were observed in coloured MPFs than in white or undyed textiles, as observed by Xue et al. (2017). Furthermore, wool contained the highest concentrations of BPs and BzPs in the current study, which compares with a study that found cotton socks contained higher BPA concentrations relative to synthetic socks (Freire et al., 2019). In contrast, Xue et al. (2017) found synthetic clothing to contain a higher concentration of BPs and BzPs relative to natural textiles. The authors indicated that this may be related to the presence of spandex in some of their test materials, where synthetic blends (polyester with 1−2% spandex) had higher additive content relative to 100% polyester. This indicates that textile composition is an important factor when assessing the environmental fate of synthetic, semi-synthetic and natural fibres. BPA has reportedly been used as a finisher in PET fibre production, though few studies investigated its occurrence in other textile types (Xue et al., 2017). It is uncertain as to why wool contained the highest median BPA concentration (501 ng/g), as no evidence concerning the use of BPA in the processing of wool fibres was identified. The next most abundant BP in MPFs and wool was BPS, with the median concentrations ranging between 0.43 and 1.95 ng/g. BPS is a common replacement chemical for BPA and therefore was expected to be present in test MPFs.

BPs and BzPs were not detected in the 5- and 10-month UV leachates or in the leachates from the high MPF concentration 14-day studies. Apart from BPA, all BPs and BzPs were present in pristine MPFs and wool fibres at low concentrations (BPAF: <LOD−1.28; bisphenol AP, BPAP: <LOD−5.49; BPF: <LOD−62.8; bisphenol P, BPP: < LOD−0.07; BPS: <LOD−2.65; BzP-1: <LOD−10.1; BzP-3: 3.29−27.7 and 4-OH-BzP: <LOD−3.55 ng/g), which explains the apparent lack of additive leaching. BPs and BzPs were shown to leach from plastic materials, although these studies were often conducted at higher temperatures or with materials containing a high proportion of additives (Sajiki and Yonekubo, 2003; Tan and Mustafa, 2003). MPFs used in 14-day leachate
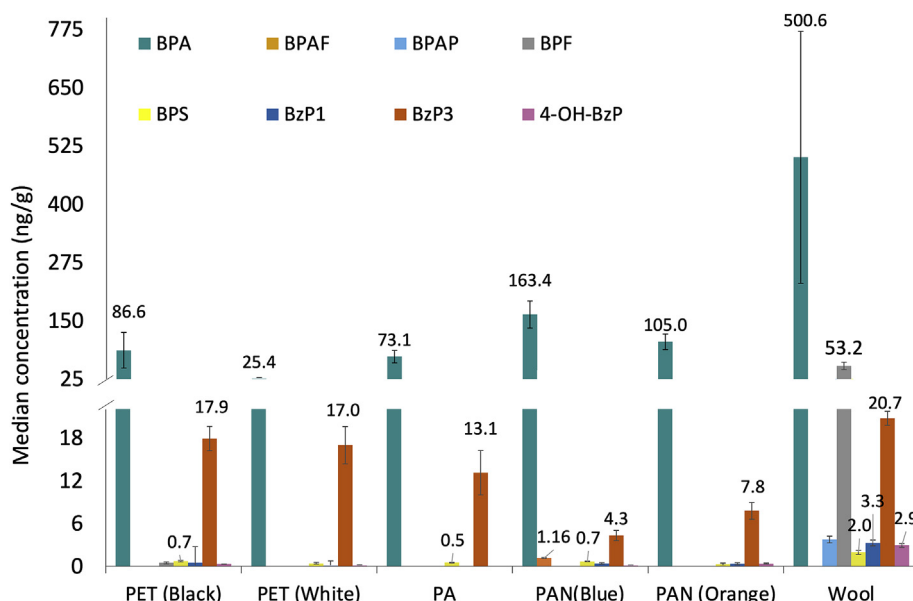

Fig. 3. Median concentration of target bisphenols and benzophenone UV filters in study MPFs and wool (n=3).

studies were ~5 mm in length, larger than the length range (1−2.5 mm) used in the UV exposure studies, the lower surface area or slower leaching rate may explain the absence of BPA. BPA was shown to undergo photodegradation under simulated environmental conditions (Sajiki and Yonekubo, 2003), suggesting any BPA leaching from the MPFs or wools fibres in UV exposed leachates may have photodegraded and was no longer detectable. The low fibre concentration used in the UV exposure studies (1 mg MPF mL^{-1}) was chosen to increase the environmental relevance but could also explain the lack of detectable leaching of BPA and other target analytes.

The identification of BzPs in the pristine MPF and wool materials suggests they may be added to the fibre as UV stabilisers to increase the durability of the final textiles. Although it was not a specific goal of the current study to assess the relationship between UV stabiliser content and the level of UV degradation observed for MPFs, we hypothesise that this group of additive chemicals may play a key role. UV stabilisers act by adsorbing the UV wavelengths, protecting the surrounding polymer, but being consumed in the process. It is therefore possible that degradation profiles of MPFs containing UV stabilisers may experience a significant delay until the additive is fully consumed. We suggest that this should be a focus of future studies, alongside investigating the role of degradation in the release of other additive chemicals present in MPFs.

4. Conclusions

PET and PA MPFs significantly fragment and undergo changes in surface morphology following up to 10 months UV exposure, with PA also exhibiting alterations in surface chemistry. Conversely, no degradation of PAN was observed in the same exposure period. Corresponding monomers, UV stabilisers and degradation products were observed in both MPFs and their leachates following exposure in water. Interestingly, wool fibres displayed higher BP and BzP content than synthetic fibres. Given the greater extent of degradation observed for PET and PA, it is proposed that faster degradation rates are a desirable property in synthetic textiles, resulting in fewer interactions or potential exposures with aquatic biota before complete remineralisation occurs. Further research is necessary to elucidate the extent to which chemical additive content and MPF composition is driving degradation. Similar changes in length, morphology and polymer chemistry between seawater and freshwater conditions imply that relative salinity does not play a significant role in the rate of photodegradation in test MPFs. However, salinity may influence additive chemical leaching. Further research investigating the degradation of wool in combination with other natural and semi-synthetic fibres is necessary to determine if MPFs pose a greater risk than other fibre types. This study demonstrates the importance of environmental parameters and material-specific properties in understanding the degradative fate of MPFs in aquatic environments.

Credit author statement

Shannen Thora Lea Sait: Data curation, Formal analysis, Investigation, Methodology, Software, Validation, Visualization, Writing - original draft., Lisbet Sørensen: Conceptualization, Investigation, Data curation, Methodology, Project administration, Resources, Supervision, Software, Validation, Writing - review & editing. Stephan Kubowicz: Methodology, Validation, Writing - review & editing. Kristine Vike-Jonas: Data curation, Investigation, Methodology, Software, Validation, Writing - review & editing., Susana Villa Gonzalez: Investigation, Methodology, Resources, Supervision, Writing - review & editing., Alexandros G. Asimakopoulos: Conceptualization, Funding acquisition, Methodology, Project administration, Resources, Supervision, Validation, Writing - review & editing. Andy M. Booth: Conceptualization, Funding acquisition, Methodology, Project administration, Resources, Supervision, Validation, Writing - review & editing.

Declaration of competing interest

The authors declare that they have no known competing financial interests or personal relationships that could have appeared to influence the work reported in this paper.

Acknowledgements

Appendix A. Supplementary data

Supplementary data to this article can be found online at https://doi.org/10.1016/j.envpol.2020.115745.

References

Aggour, Y.A., Aziz, M.S., 2000. Degradation of polyacrylonitrile by low energy ion beam and UV radiation. Polym. Test. 19, 261−267. https://doi.org/10.1016/S0142-9418(98)00087-7.

Allen, N.S., Edge, M., 1992. Fundamentals of Polymer Degradation and Stabilisation. Elsevier Applied Science, London, New York.

Andrady, A.L., 2011. Microplastics in the marine environment. Mar. Pollut. Bull. 62, 1596−1605. https://doi.org/10.1016/j.marpolbul.2011.05.030.

Andrady, A.L. (Ed.), 2003. Plastics and the Environment. Wiley-Interscience, Hoboken, N.J.

Arctander, S., 2019. Perfume & Flavor Chemicals (Aroma Chemicals) Vol. II. Lulu. com.

Armstrong, R.D., Jenkins, A.T.A., Johnson, B.W., 1995. An investigation into the uv breakdown of thermoset polyester coatings using impedance spectroscopy. Corrosion Sci. 37, 1615−1625. https://doi.org/10.1016/0010-938X(95)00063-.

Asimakopoulos, A.G., Thomaidis, N.S., Kannan, K., 2014a. Widespread occurrence of bisphenol A diglycidyl ethers, p-hydroxybenzoic acid esters (parabens), benzophenone type-UV filters, triclosan, and triclocarban in human urine from Athens, Greece. Sci. Total Environ. 470−471, 1243−1249. https://doi.org/10.1016/j.scitotenv.2013.10.089.

Asimakopoulos, A.G., Wang, L., Thomaidis, N.S., Kannan, K., 2014b. A multi-class bioanalytical methodology for the determination of bisphenol A diglycidyl ethers, p-hydroxybenzoic acid esters, benzophenone-type ultraviolet filters, triclosan, and triclocarban in human urine by liquid chromatography−tandem mass spectrometry. J. Chromatogr. A 1324, 141−148. https://doi.org/10.1016/j.chroma.2013.11.031.

Barrows, A.P.W., Cathey, S.E., Petersen, C.W., 2018. Marine environment microfiber contamination: global patterns and the diversity of microparticle origins. Environ. Pollut. 237, 275−284. https://doi.org/10.1016/j.envpol.2018.02.062.

Capolupo, M., Sørensen, L., Jayasena, K.D.R., Booth, A.M., Fabbri, E., 2020. Chemical composition and ecotoxicity of plastic and car tire rubber leachates to aquatic organisms. Water Res. 169, 115270. https://doi.org/10.1016/j.watres.2019.115270.

Carney Almroth, B.M., Åström, L., Roslund, S., Petersson, H., Johansson, M., Persson, N.-K., 2018. Quantifying shedding of synthetic fibers from textiles; a source of microplastics released into the environment. Environ. Sci. Pollut. Res. 25, 1191−1199. https://doi.org/10.1007/s11356-017-0528-7.

Cesa, F.S., Turra, A., Checon, H.H., Leonardi, B., Baruque-Ramos, J., 2020. Laundering and textile parameters influence fibers release in household washings. Environ. Pollut. 257, 113553. https://doi.org/10.1016/j.envpol.2019.113553.

Chandure, A.S., Bhusari, G.S., Umare, S.S., 2014. Synthesis, characterization, and

biodegradation studies of poly(1,4-cyclohexanedimethylene-adipate-carbonate)s. J. Polym. 1–11. https://doi.org/10.1155/2014/547325.

Chequer, F.M.D., Oliveira, G.A.R. de, Ferraz, E.R.A., Cardoso, J.C., Zanoni, M.V.B., Oliveira, D.P. de, 2013. Textile dyes: dyeing process and environmental impact. Eco-friendly text. Dye. Finish. https://doi.org/10.5772/53659.

Cole, M., 2016. A novel method for preparing microplastic fibers. Sci. Rep. 6 https://doi.org/10.1038/srep34519.

Cole, M., Coppock, R., Lindeque, P.K., Altin, D., Reed, S., Pond, D.W., Sørensen, L., Galloway, T.S., Booth, A.M., 2019. Effects of nylon microplastic on feeding, lipid accumulation, and moulting in a coldwater copepod. Environ. Sci. Technol. 53, 7075–7082. https://doi.org/10.1021/acs.est.9b01853.

Corradini, F., Meza, P., Eguiluz, R., Casado, F., Huerta-Lwanga, E., Geissen, V., 2019. Evidence of microplastic accumulation in agricultural soils from sewage sludge disposal. Sci. Total Environ. 671, 411–420. https://doi.org/10.1016/j.scitotenv.2019.03.368.

Da Costa, J.P., Nunes, A.R., Santos, P.S.M., Girão, A.V., Duarte, A.C., Rocha-Santos, T., 2018. Degradation of polyethylene microplastics in seawater: insights into the environmental degradation of polymers. J. Environ. Sci. Health Part A Tox. Hazard. Subst. Environ. Eng. 53, 866–875. https://doi.org/10.1080/10934529.2018.1455381.

Darbra, R.M., Dan, J.R.G., Casal, J., Àgueda, A., Capri, E., Fait, G., Schuhmacher, M., Nadal, M., Rovira, J., Grundmann, V., Barceló, D., Ginebreda, A., Guillén, D., 2012. Additives in the textile industry. In: Bilitewski, B., Darbra, Rosa Mari, Barceló, Damià (Eds.), Global Risk-Based Management of Chemical Additives I: Production, Usage and Environmental Occurrence, the Handbook of Environmental Chemistry. Springer, Berlin, Heidelberg, pp. 83–107. https://doi.org/10.1007/698_2011_101.

Dawson, A.L., Kawaguchi, S., King, C.K., Townsend, K.A., King, R., Huston, W.M., Nash, S.M.B., 2018. Turning microplastics into nanoplastics through digestive fragmentation by Antarctic krill. Nat. Commun. 9, 1001. https://doi.org/10.1038/s41467-018-03465-9.

De Falco, F., Gullo, M.P., Gentile, G., Di Pace, E., Cocca, M., Gelabert, L., Brouta-Agnésa, M., Rovira, A., Escudero, R., Villalba, R., Mossotti, R., Montarsolo, A., Gavignano, S., Tonin, C., Avella, M., 2018. Evaluation of microplastic release caused by textile washing processes of synthetic fabrics. Environ. Pollut. 236, 916–925. https://doi.org/10.1016/j.envpol.2017.10.057.

Deterre, R., Feller, J.-F., Hamaide, T., 2014. Environmental Impact of Polymers. ISTE, Ltd. ; Wiley, London; Hoboken.

Freeman, S., Booth, A.M., Sabbah, I., Tiller, R., Dierking, J., Klun, K., Rotter, A., Ben-David, E., Javidpour, J., Angel, D.L., 2020. Between source and sea: the role of wastewater treatment in reducing marine microplastics. J. Environ. Manag. 266, 110642. https://doi.org/10.1016/j.jenvman.2020.110642.

Freire, C., Molina-Molina, J.-M., Iribarne-Durán, L.M., Jiménez-Díaz, I., Vela-Soria, F., Mustieles, V., Arrebola, J.P., Fernández, M.F., Artacho-Cordón, F., Olea, N., 2019. Concentrations of bisphenol A and parabens in socks for infants and young children in Spain and their hormone-like activities. Environ. Int. 127, 592–600. https://doi.org/10.1016/j.envint.2019.04.013.

Frick, E., Ernst, H.A., Voll, D., Wolf, T.J.A., Unterreiner, A.-N., Barner-Kowollik, C., 2014. Studying the polymerization initiation efficiency of acetophenone-type initiators via PLP-ESI-MS and femtosecond spectroscopy. Polym. Chem. 5, 5053–5068. https://doi.org/10.1039/C4PY00418C.

Gewert, B., Plassmann, M., Sandblom, O., MacLeod, M., 2018. Identification of chain scission products released to water by plastic exposed to ultraviolet light. Environ. Sci. Technol. Lett. 5, 272–276. https://doi.org/10.1021/acs.estlett.8b00119.

Gewert, B., Plassmann, M.M., MacLeod, M., 2015. Pathways for degradation of plastic polymers floating in the marine environment. Environ. Sci. Process. Impacts 17, 1513–1521. https://doi.org/10.1039/C5EM00207A.

Hermabessiere, L., Dehaut, A., Paul-Pont, I., Lacroix, C., Jezequel, R., Soudant, P., Duflos, G., 2017. Occurrence and effects of plastic additives on marine environments and organisms: a review. Chemosphere 182, 781–793. https://doi.org/10.1016/j.chemosphere.2017.05.096.

Ioakeimidis, C., Fotopoulou, K.N., Karapanagioti, H.K., Geraga, M., Zeri, C., Papathanassiou, E., Galgani, F., Papatheodorou, G., 2016. The degradation potential of PET bottles in the marine environment: an ATR-FTIR based approach. Sci. Rep. 6 https://doi.org/10.1038/srep23501.

Jellinek, H.H.G., Bastien, I.J., n.d. PHOTOLYSIS OF POLYACRYLONITRILE 13.

Jellinek, H.H.G., Schlueter, W.A., 1960. Photodegradation of polyacrylonitrile in solution. J. Appl. Polym. Sci. 3, 206–212. https://doi.org/10.1002/app.1960.070030810.

Karlsson, T.M., Hassellöv, M., Jakubowicz, I., 2018. Influence of thermooxidative degradation on the in situ fate of polyethylene in temperate coastal waters. Mar. Pollut. Bull. 135, 187–194. https://doi.org/10.1016/j.marpolbul.2018.07.015.

Koelmans, A.A., Mohamed Nor, N.H., Hermsen, E., Kooi, M., Mintenig, S.M., De France, J., 2019. Microplastics in freshwaters and drinking water: critical review and assessment of data quality. Water Res. 155, 410–422. https://doi.org/10.1016/j.watres.2019.02.054.

Ksouri, I., Haddar, N., 2018. Long term ageing of polyamide 6 and polyamide 6 reinforced with 30% of glass fibers: temperature effect. J. Polym. Res. 25, 153. https://doi.org/10.1007/s10965-018-1551-1.

Lenzing, A.G., 2017. Annual Report 2017.

Mason, S.A., Garneau, D., Sutton, R., Chu, Y., Ehmann, K., Barnes, J., Fink, P., Papazissimos, D., Rogers, D.L., 2016. Microplastic pollution is widely detected in US municipal wastewater treatment plant effluent. Environ. Pollut. 218, 1045–1054. https://doi.org/10.1016/j.envpol.2016.08.056.

Mintenig, S.M., Int-Veen, I., Löder, M.G.J., Primpke, S., Gerdts, G., 2017. Identification of microplastic in effluents of waste water treatment plants using focal plane array-based micro-Fourier-transform infrared imaging. Water Res. 108, 365–372. https://doi.org/10.1016/j.watres.2016.11.015.

Murphy, F., Ewins, C., Carbonnier, F., Quinn, B., 2016. Wastewater treatment works (WwTW) as a source of microplastics in the aquatic environment. Environ. Sci. Technol. 50, 5800–5808. https://doi.org/10.1021/acs.est.5b05416.

Napper, I.E., Thompson, R.C., 2016. Release of synthetic microplastic plastic fibres from domestic washing machines: effects of fabric type and washing conditions. Mar. Pollut. Bull. 112, 39–45. https://doi.org/10.1016/j.marpolbul.2016.09.025.

n.d National Center for Biotechnology Information PubChem Database. Ethyl 4-ethoxybenzoate, CID=90232 [WWW Document]. Ethyl 4-Ethoxybenzoate CID90232 (accessed 4.15.20). https://pubchem.ncbi.nlm.nih.gov/compound/Ethyl-4-ethoxybenzoate.

Nizzetto, L., Futter, M., Langaas, S., 2016. Are agricultural soils dumps for microplastics of urban origin? Environ. Sci. Technol. 50, 10777–10779. https://doi.org/10.1021/acs.est.6b04140.

OECD, 2011. Test No. 201: Freshwater Alga and Cyanobacteria, Growth Inhibition Test. https://doi.org/10.1787/9789264069923-en.

Parvinzadeh, M., Ebrahimi, I., 2011. Influence of atmospheric-air plasma on the coating of a nonionic lubricating agent on polyester fiber. Radiat. Eff. Defect Solid 166, 408–416. https://doi.org/10.1080/10420150.2011.553230.

Patty, D.J., Loupatty, G., Sopalauw, F., 2017. Interpretation FTIR spectrum of seawater and sediment in the Ambon Bay (TAD). In: AIP Conference Proceedings. AIP Publishing LLC, 060005.

Porubská, M., Szöllős, O., Kóňová, A., Janigová, I., Jašková, M., Jomová, K., Chodák, I., 2012. FTIR spectroscopy study of polyamide-6 irradiated by electron and proton beams. Polym. Degrad. Stabil. 97, 523–531. https://doi.org/10.1016/j.polymdegradstab.2012.01.017.

Random Integer Generator, 1998 [WWW Document](accessed 5.13.19). https://www.random.org/integers/.

Revel, M., Châtel, A., Mouneyrac, C., 2018. Micro(nano)plastics: a threat to human health? Curr. Opin. Environ. Sci. Health 1, 17–23. https://doi.org/10.1016/j.coesh.2017.10.003.

Ribeiro, R.F., Pardini, L.C., Alves, N.P., Brito Júnior, C.A.R., Ribeiro, R.F., Pardini, L.C., Alves, N.P., Brito Júnior, C.A.R., 2015. Thermal Stabilization study of poly-acrylonitrile fiber obtained by extrusion. Polímeros 25, 523–530. https://doi.org/10.1590/0104-1428.1938.

Rouillon, C., Bussiere, P.-O., Desnoux, E., Collin, S., Vial, C., Therias, S., Gardette, J.-L., 2016. Is carbonyl index a quantitative probe to monitor polypropylene photo-degradation? Polym. Degrad. Stabil. 128, 200–208. https://doi.org/10.1016/j.polymdegradstab.2015.12.011.

Rummel, C.D., Escher, B.I., Sandblom, O., Plassmann, M.M., Arp, H.P.H., MacLeod, M., Jahnke, A., 2019. Effects of leachates from UV-weathered microplastic in cell-based bioassays. Environ. Sci. Technol. 53, 9214–9223. https://doi.org/10.1021/acs.est.9b02400.

Sajiki, J., Yonekubo, J., 2003. Leaching of bisphenol A (BPA) to seawater from polycarbonate plastic and its degradation by reactive oxygen species. Chemosphere 51, 55–62. https://doi.org/10.1016/S0045-6535(02)00789-0.

Sathish, N., Jeyasanta, K.I., Patterson, J., 2019. Abundance, characteristics and surface degradation features of microplastics in beach sediments of five coastal areas in Tamil Nadu, India. Mar. Pollut. Bull. 142, 112–118. https://doi.org/10.1016/j.marpolbul.2019.03.037.

Schneider, C.A., Rasband, W.S., Eliceiri, K.W., 2012. NIH Image to ImageJ: 25 years of image analysis. Nat. Methods 9, 671–675. https://doi.org/10.1038/nmeth.2089.

Tan, B.L.L., Mustafa, A.M., 2003. Leaching of bisphenol A from new and old babies' bottles, and new babies' feeding teats. Asia Pac. J. Publ. Health 15, 118–123. https://doi.org/10.1177/101053950301500208.

Thanki, P.N., Singh, R.P., 1998. Photo-oxidative degradation of nylon 66 under accelerated weathering. Polymer 39, 6363–6367. https://doi.org/10.1016/S0032-3861(97)10390-1.

Vahur, S., Teearu, A., Peets, P., Joosu, L., Leito, I., 2016. ATR-FT-IR spectral collection of conservation materials in the extended region of 4000-80 cm−1. Anal. Bioanal. Chem. 408, 3373–3379. https://doi.org/10.1007/s00216-016-9411-5.

Wang, L., Zhang, Y., Liu, Y., Gong, X., Zhang, T., Sun, H., 2019. Widespread occurrence of bisphenol A in daily clothes and its high exposure risk in humans. Environ. Sci. Technol. 53, 7095–7102. https://doi.org/10.1021/acs.est.9b02090.

Wang, Z., Chen, M., Zhang, L., Wang, K., Yu, X., Zheng, Z., Zheng, R., 2018. Sorption behaviors of phenanthrene on the microplastics identified in a mariculture farm in Xiangshan Bay, southeastern China. Sci. Total Environ. 628, 1617–1626.

Weedon, G.C., Decaprio, J.D., 1971. Prevention of Yellowing in Polyamides.

Xue, J., Liu, W., Kannan, K., 2017. Bisphenols, benzophenones, and bisphenol A diglycidyl ethers in textiles and infant clothing. Environ. Sci. Technol. 51, 5279–5286. https://doi.org/10.1021/acs.est.7b00701.

Zambrano, M.C., Pawlak, J.J., Daystar, J., Ankeny, M., Cheng, J.J., Venditti, R.A., 2019. Microfibers generated from the laundering of cotton, rayon and polyester based fabrics and their aquatic biodegradation. Mar. Pollut. Bull. 142, 394–407. https://doi.org/10.1016/j.marpolbul.2019.02.062.

Zambrano, M.C., Pawlak, J.J., Daystar, J., Ankeny, M., Goller, C.C., Venditti, R.A., 2020. Aerobic biodegradation in freshwater and marine environments of textile microfibers generated in clothes laundering: effects of cellulose and polyester-based microfibers on the microbiome. Mar. Pollut. Bull. 151, 110826. https://doi.org/10.1016/j.marpolbul.2019.110826.

Zhang, L., Xie, Y., Liu, J., Zhong, S., Qian, Y., Gao, P., 2020. An overlooked entry pathway of microplastics into agricultural soils from application of sludge-

based fertilizers. Environ. Sci. Technol. 54, 4248−4255. https://doi.org/10.1021/acs.est.9b07905.

Zhang, S., Zhang, J., Tang, L., Huang, J., Fang, Y., Ji, P., Wang, C., Wang, H., 2019. A novel synthetic strategy for preparing polyamide 6 (PA6)-Based polymer with transesterification. Polymers 11, 978.

Zimmermann, L., Dierkes, G., Ternes, T.A., Völker, C., Wagner, M., 2019. Benchmarking the in vitro toxicity and chemical composition of plastic consumer products. Environ. Sci. Technol. 53, 11467−11477. https://doi.org/10.1021/acs.est.9b02293.